WATER RESOURCES RESEARCH, VOL. 33, NO. 3, PAGES 419–426, MARCH 1997

Synthesizing shallow seasonal snow covers

K. Shook and D. M. Gray

Division of Hydrology, College of Engineering, University of Saskatchewan, Saskatoon, Saskatchewan, Canada

Abstract. A method of synthesizing a snowfield from point field measurements, which is based on the fractal structure of the water equivalent, is presented. Two steps are involved in the synthesis. First, the method of fractal sum of pulses is used to generate the spatial distribution of the snow water equivalent in an array. Second, the synthetic snowfield is adjusted to take on the statistical properties of the natural snow cover. The two-parameter lognormal probability density function fitted to field data is used for this purpose. Examples of the application of the lognormal distribution for describing the water equivalent of snow covers on various landscapes encountered in a prairie environment are presented. The geometrical properties (fractal dimension(s)) of snow patches that result from melting a synthetic snow cover agree closely with those of patches of an ablated natural snow cover.

1. Introduction

Information on the spatial distribution of the water equivalent of a snow cover is required for accurate predictions of melt and runoff. In addition to governing the mass of water contained by a snow cover, which potentially may form runoff, the spatial distribution of the snow cover water equivalent affects the geometry of the snow-covered area of a basin at various stages of ablation. The last is extremely important in environments with shallow seasonal snow covers, which on melting disintegrate into a mosaic of patches of snow and bare ground. The extent of the gross area of a watershed that is snow-covered affects runoff primarily in two ways: (1) it influences the melt rate, and (2) it governs the contributing area of runoff. The lower albedo of the patches of bare ground changes the radiation balance from that for a complete snow cover and local advection of energy from the snow-free areas becomes increasingly important to melt. Melting of patches of snow occurs at a maximum rate along the leading edge of snow and decreases exponentially with increasing fetch. Throughout ablation the relative importance of radiation and turbulent energy sources to melt depend on the size and patchiness of the snowfield. Small patches of snow are dominated by turbulent melt until they disappear, whereas large, extensive snow fields are dominated by radiation melt early in the season and turbulent melt late in the season as they decrease in area. The highest rate of meltwater production in a watershed is most likely to occur when the product of the average melt rate and snow-covered area is a maximum.

An areal depletion curve is often used to correct quantities of melt and runoff, which are calculated assuming complete snow cover on a basin, for the fraction of the basin area that is snow-covered. The *U.S. Army Corps of Engineers* [1956], *Anderson* [1973], and *Martinec* [1980, 1985] describe depletion curves that use the mean water equivalent of a "complete" snow cover for modeling the process. *Dunne and Leopold* [1978], *Ferguson* [1984], and *Buttle and McDonnell* [1987], modeled snow coverage at various stages of melt on a basin by applying one-dimensional melt rates to the frequency distribution of the water equivalent. This approach is limited because one-dimensional models cannot describe physically those melt processes that are truly two-dimensional in nature. For example, the effects on melt of local advection, changes in the geometry of the soil and snow patches, changes in the albedo of snow because of metamorphism, or changes to the energetics of snowmelt due to the penetration of solar radiation through snow to the underlying ground. Because patchy snow cover has a two-dimensional structure, a model of the ablation of these snow covers should be at least two-dimensional.

Shook [1993, 1995], *Shook et al.* [1993a, b], and *Shook and Gray* [1997] show that (1) the spatial distribution of snow depth and water equivalent is fractal at small scales and random at large scales; (2) the patches of soil and snow that form during the ablation of shallow seasonal snow covers may be considered fractal objects; that is, their perimeter and size-frequency characteristics may be described by simple power functions of patch area; (3) the fractal properties of soil and snow patches are due to the fractal structure of the water equivalent of the snow cover; and (4) a two-dimensional melt model, which synthesizes local advection, applied to an array having the fractal spatial distribution of the snow water equivalent, produces ablated snow covers with fractal properties similar to those found in nature. These findings offer the potential for developing a physically based algorithm for simulating melting of shallow, patchy snow covers.

An obstacle to the development of such a model is the requirement for sufficient data to define accurately the character and spatial distribution of the snow water equivalent. Field estimates of the water equivalent of a snow cover frequently are calculated from measurements of snow depth and density. In practice, fewer measurements of density are taken than those of depth because of the effort required for the density measurement. Therefore the number of density samples usually constrains the number of data points for analyses. An alternative to increased sampling, which would be less time-consuming and less expensive, is to generate a synthetic snowfield and adjust the data to take on properties of the natural snow field based on field samples. Generating water equivalent data has several advantages: (1) it allows the modeler to create the amount of data required, (2) the behavior of the snowpack may be correlated with the variation in the

Paper number 96WR03532.
0043-1397/97/96WR-03532$09.00

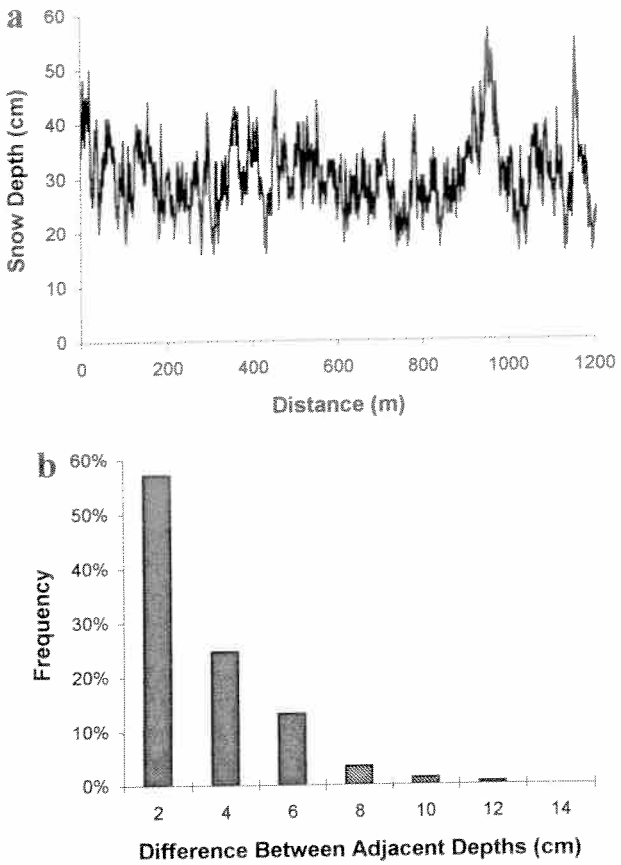

Figure 1. Variation in snow depth on a relatively flat field of wheat stubble in a prairie environment: (a) snow depth along a transect and (b) frequency distribution of the differences between snow depth at adjacent measurement points along transect.

model data, and (3) the number of field samples required for modeling may be reduced.

This paper describes a procedure for generating a synthetic snow cover that forms soil and snow patches having fractal properties similar to those of an ablated natural snow cover. Initially, the water equivalent of a snow field is generated by a technique called the fractal sum of pulses [*Lovejoy and Mandelbrot*, 1985]. Then, using field observations, the synthetic data are adjusted to take on characteristics of a natural snow cover. The perimeter-area and size-frequency characteristics of snow patches of ablated synthetic and natural snow covers field are shown to agree closely.

2. Properties of the Water Equivalent of Natural Shallow Prairie Snow Covers

Over characteristic distances less than 100 m (microscale), differences in accumulation patterns of snow covers in open, prairie regions result from variations in air flow patterns and snow transport. In addition to atmospheric variables, the primary factors affecting snow accumulation are surface roughness, terrain features, and snow supply and erodability. Even along a snow course that traverses large differences in vegetation and topography, snow depth and water equivalent at adjacent sampling points may exhibit high autocorrelation. Figure 1a shows a cross section of snow depths measured at 1-m intervals on a relatively flat field of wheat stubble at Saskatoon, Saskatchewan, Canada. Figure 1b plots the frequency distribution of the differences between snow depths at adjacent sampling points in the transect. The distribution is exponential and the large number of small differences in depth reflects the high autocorrelation between measurements.

Shook [1995] and *Shook and Gray* [1997] showed that because of autocorrelation, the spatial variation of snow depth in open, exposed prairie and arctic environments is fractal at small scales, becoming random at scales beyond some limiting length. For an evenly sampled fractal series, positive autocorrelation causes the standard deviation(s) to be a power function of sample size (T) [*Turcotte*, 1992],

$$s \propto T^{H}, \tag{1}$$

where H is the Hausdorff measure (constant), equal to $2 - D$, in which D is the fractal dimension. Therefore the standard deviation changes with sampling distance. If the data are randomly distributed, the standard deviation is independent of sample size. The transition of fractal to random behavior is related to the degree of macroscopic variability of the underlying topography. The implications to snow measurement and snowmelt modeling of the variation in frequency characteristics due to the change from fractal to random behavior are discussed by *Shook* [1995] and *Shook and Gray* [1997].

Shook [1993] and *Shook et al.* [1993a] showed that the fractal properties of soil and snow patches of ablated snowcovers are the result of the spatial variation in the snowcover water equivalent (SWE). The autocorrelation of snow depth and the association between snow depth and density cause the spatial distribution in SWE to be fractal.

The average, vertically integrated density of a prairie snow cover within a specific landscape class varies only slightly during the winter [*McKay*, 1970]. *Shook and Gray* [1994] analyzed about 2400 measurements of snow depth and density of shallow seasonal snow covers taken over several years near the time of maximum accumulation on a variety of landscapes in west-central Saskatchewan, Canada. They found poor correlation between depth and density. For snow covers with a mean depth, $\bar{d}_s \leq 60$ cm, the association between variables gave $r^2 = 0.0008$, where r^2 is the coefficient of determination. Since the covariance, which is directly related to r^2, is small, the mean water equivalent can be calculated from the product of the mean snow depth and the mean density ($\approx$250 kg/m^3). Also, because the spatial variations in density are random and small, compared to variations in snow depth, the spatial distribution in water equivalent follows closely the distribution of snow depth. Figure 2, which plots the coefficients of variation of snow depth, density, and water equivalent versus sampling distance determined from measurements taken on a hummocky landscape in fallow, demonstrates these trends.

Deep prairie snow covers, that is, those with $\bar{d}_s > 60$ cm, usually result from the deposition of wind-transported snow. They are found in areas of snow accumulation, for example, within and surrounding vegetative and mechanical barriers and farm yards, in major topographical depressions such as stream channels and drainage ways, and to the lee of hills. Although these snows cover only a small fraction of the total landscape, the runoff they produce on melting may be a significant part of the annual yield, especially in low-snow years. *Shook and Gray* [1994] reported the association between density and depth for the deeper snow covers was slightly higher than that for the shallow snow with $r^2 = 0.19$. They proposed

$$\overline{SWE} = 341\bar{d}_s - 45.6, \quad (2)$$

in which $\overline{SWE}$ is in millimeters and $\bar{d}_s$ is in centimeters. The trend for the integrated density of accumulations of wind-deposited snow to increase with increasing depth is consistent with the association between variables reported by *Tabler and Schmidt* [1986] for drifts within and surrounding snow fences.

3. Synthetic Snow Covers

It is evident from the discussions above that any synthetic representation of a snowfield that is used to model the ablation of a shallow seasonal snow cover must preserve the fractal structure of the water equivalent of natural snow.

Random Generation

An early attempt to generate a synthetic snowcover assigned SWE values randomly to an array [*Shook*, 1993]. The purpose in testing this approach was to determine (1) if fractal snow patches can arise spontaneously from a random system (as a fractal can be generated randomly from the "chaos game" [*Gleick*, 1987]) and (2) if melt fluxes alone could cause an ablated snow cover to take on fractal characteristics. A typical image of an ablated, randomly generated snow cover is presented in Figure 3a. It shows a salt-and-pepper arrangement of evenly scattered black and white pixels that are nonrepresentative of the distributions of natural soil and snow patches. The flaws in this method of modeling the snow cover water equivalent are that (1) the frequency distribution of snow water equivalent is very uniform (field values of SWE follow a heap-shaped distribution) and (2) the placement of the snow water equivalents within an array is random (this results in poor autocorrelation between the depths at adjacent stations (see Figure 3b). The inability of the random assignment of snow water equivalent to produce fractal snow patches is taken to indicate that the factors causing the formation of snow patches are not random in nature and energy fluxes cannot, by themselves, form fractal snow patches.

Fractal Generation

Shook et al. [1993] demonstrated that the method of fractal sum of pulses (FSP) is capable of generating synthetic SWE data with characteristics similar to those found in natural snow covers. This technique was developed by *Lovejoy and Mandelbrot* [1985] for modeling clouds and rainfall. Sets of pulses (collections of array elements) are created. The dimensions of each pulse are determined by a biased pseudorandom process. Each array element in each pulse is assigned a value. According to *Lovejoy and Mandelbrot* [1985], it is necessary for the pulse sizes and values to be hyperbolically distributed to generate a fractal object. The pulses, which may be positive or negative, are then placed at random locations, the values of the pulse being added to the previous values of the array elements. The process is repeated for the desired number of pulses.

The FSP process used to synthesize a snow cover placed "cylinders," that is, round collections of elements, in the array. In keeping with Lovejoy and Mandelbrot's algorithms, both the diameters and the heights (the SWE values) have hyperbolic distributions. *Shook* [1993] provides a program listing for this algorithm. By varying the number of pulses, the maximum pulse radius, the exponent of the relationship between hyperbolic diameter and depth, and the ratio of cylinder height to radius, snowpacks having different spatial distributions can be generated.

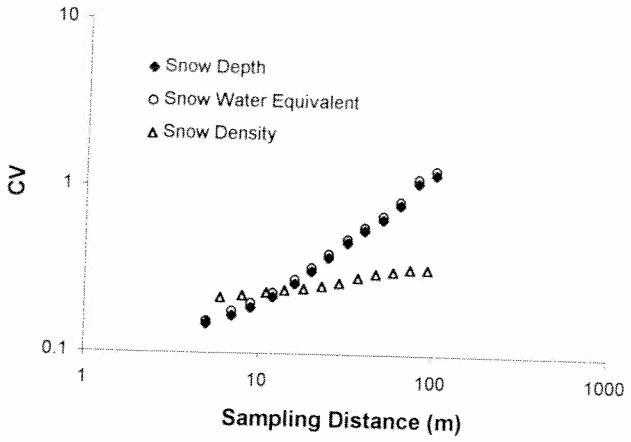

Figure 2. Variations in the coefficients of variation of snow depth, density, and water equivalent with sampling distance determined from field observations on a hummocky field in fallow near Saskatoon, Saskatchewan, Canada.

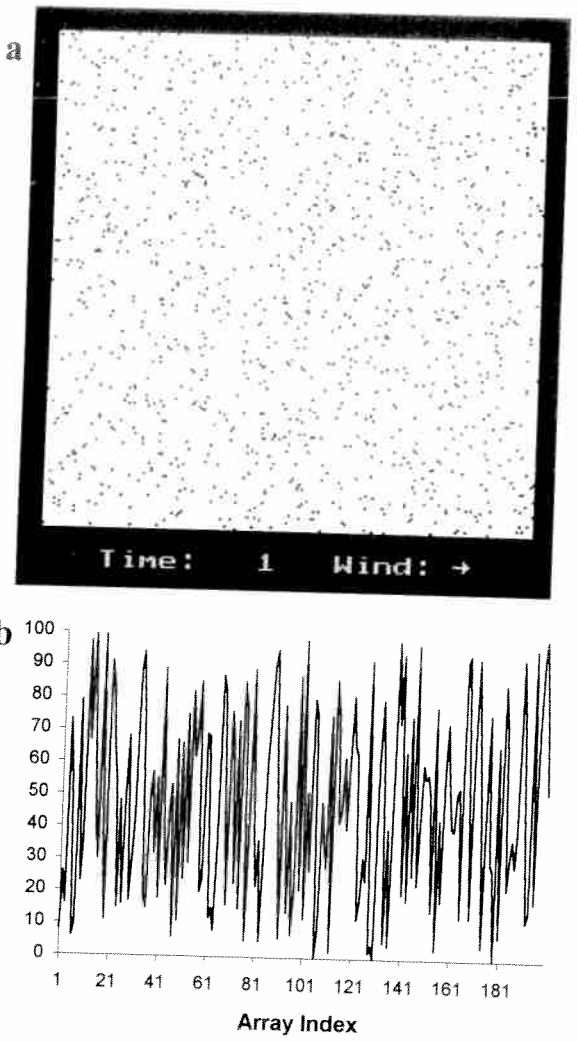

Figure 3. Characteristics of synthetic snow covers by random generation: (a) image of a melting snow cover, and (b) variation in water equivalent along a transect.

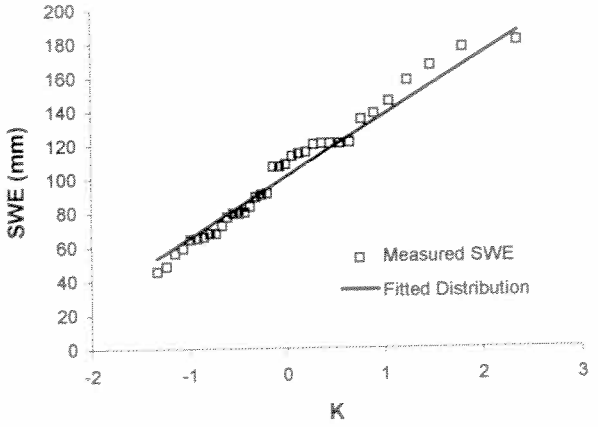

Figure 4. Point measurements of snow cover water equivalent from a relatively flat field of wheat stubble fitted to a lognormal distribution.

Adjusting a Synthetic SWE Frequency Distribution

An inherent deficiency of the FSP method of generating a snowpack is that the modeler has limited control over the frequency characteristics of the snowfield that is created. Therefore it is necessary to adjust the synthetic snowfield to take on frequency characteristics of the snow cover that is being modeled. The following information and steps are used to accomplish this: (1) an estimate, determined by field measurements, of the frequency characteristics of the water equivalent of the natural snow cover, (2) measurement of the frequency distribution of the water equivalent of the synthetic snow cover, and (3) conversion of the SWE distribution of the synthetic snow cover to that of the natural snow cover.

Use of the lognormal probability density function to describe the frequency distribution of the SWE of a natural snow cover. The two-parameter lognormal probability density function is used to describe the frequency distribution of the water equivalent. In linear form it is

$$\mathrm{SWE} = \overline{\mathrm{SWE}}(1 + K \times \mathrm{CV}) \tag{3}$$

or

$$\mathrm{SWE} = \overline{\mathrm{SWE}} + Ks, \tag{4}$$

where

SWE natural value of the snow water equivalent having an exceedance probability equal to that of the frequency factor, K [*Chow*, 1954];

$\overline{\mathrm{SWE}}$ arithmetic mean of the natural values;

CV coefficient of variation of the natural values;

s standard deviation of the natural values.

Figures 4, 5, and 6 are representative plots of point measurements of water equivalent and fitted distributions for: (1) a relatively flat field in wheat stubble (Figure 4), (2) an undulating field of fallow (Figure 5) and (3) a relatively flat low area with scattered brush (Figure 6). The respective coefficients of determination, r^2, between the measured and fitted SWE values for the three landscapes are 0.92, 0.98, and 0.99, respectively.

Variation in coefficient of variation of snow water equivalent with landscape class. At large (field) scales within relatively homogeneous climatic regions of the Canadian prairies, the spatial distribution of the water equivalent of a snow cover is strongly influenced by vegetation and topography. *McKay* [1970] and *Steppuhn and Dyck* [1974] found that stratifying a watershed according to terrain and vegetative variables, then sampling snow covers of the same landscape class, reduced the coefficient of variation of SWE. Table 1 lists representative values for CV of snow cover water equivalent for various landscapes within a prairie environment. They summarize the results of analyses of snow survey data collected on various landscape units in 3 years of varying snowfall amounts. All snow measurements were made in late winter, near a time of maximum accumulation of the seasonal snow cover and before significant melting had occurred.

The trends exhibited by the data are consistent with findings reported in the literature [e.g., *Woo and Marsh*, 1977] and field observations:

1. The variability in water equivalent is greater on fallow land than on land with a vegetative cover.
2. Vegetation dampens the variability in water equivalent due to landform. The denser the vegetation, the greater the effect. For example, a common $\mathrm{CV}_{\mathrm{SWE}}$ can be used to describe the frequency distribution of water equivalent of snowcover on most landforms encountered in the prairie environment that are covered with the stubble of a closely seeded cereal grain or pulse crop.

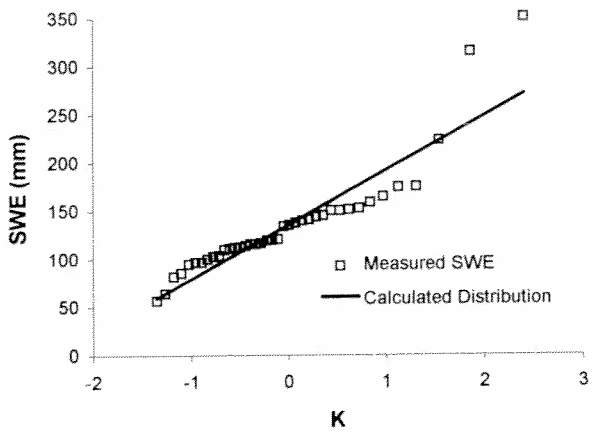

Figure 5. Point measurements of snow cover water equivalent from an undulating field of fallow fitted to a lognormal distribution.

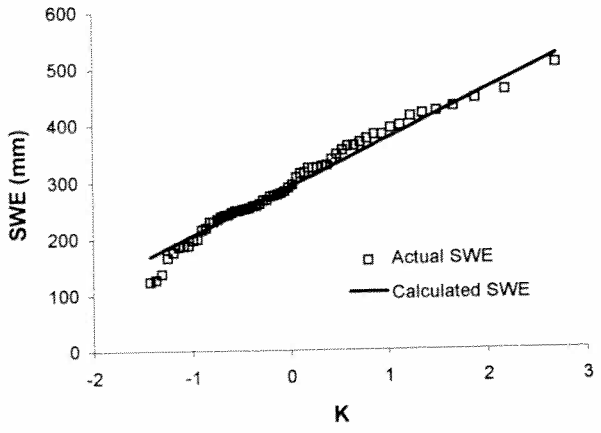

Figure 6. Point measurements of snow cover water equivalent from relatively flat low land in scattered brush fitted to a lognormal distribution.

3. Snow accumulation patterns are affected mainly by those topographic features that cause major divergence in air flow patterns, that is, snow erosion and deposition. This is reflected in the larger values of the coefficient of variation for the crests of hills and the lee of abrupt slopes.

Where field measurements of the mean and standard deviation of the water equivalent of a snow cover are not available, the values for CV_{SWE} in Table 1 can be used as first approximations. Estimates of CV_{SWE} determined from direct field measurements may vary appreciably around these representative values. First, the landscape classification is qualitative and subjective. Second, land use and landform features are not mutually independent. For example, steep slopes, deep gullies and sloughs (if wet) are not cultivated and support the growth of riparian vegetation, such as native grasses and scattered brush. Third, CV_{SWE} will vary with factors other than landscape features, for example, with differences in processes affecting snow metamorphism, snowfall distribution, redistribution of snow by wind, and sample size.

The effects of variations in CV_{SWE} on the depletion in snow-covered area are shown in Figure 7. For these simulations the initial mean snow water equivalent at the start of melt was assumed to be constant. The results demonstrate that the smaller the value of CV_{SWE}, the more rapid the depletion. This is to be expected because the peakedness of the frequency distribution of SWE increases with decreasing CV_{SWE}. Therefore the smaller the coefficient of variation, the larger the number of SWE values clustered close to the mean.

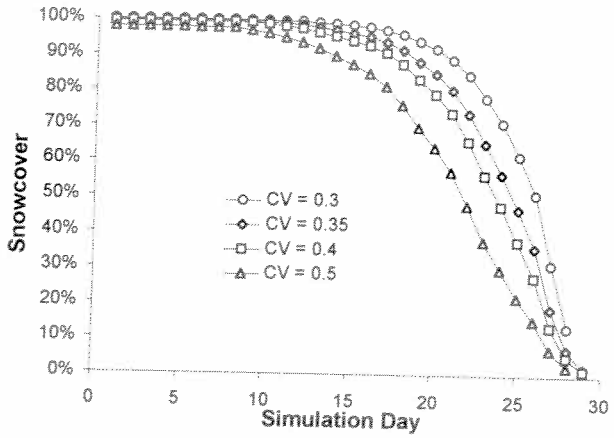

Figure 7. Effect of the coefficient of variation of water equivalent on snow cover depletion.

Adjustment Procedure

Adjustment of a synthetic snowfield to take on statistical properties of a natural snowfield involves using (3) or (4) with the same frequency factor for synthetic and measured values. This leads to the expression

$$SWE_a = s_m\left(\frac{SWE_s - \overline{SWE_s}}{S_s}\right) + \overline{SWE_m}, \qquad (5)$$

in which SWE_a is the adjusted water equivalent and the subscripts m and s refer to the measured (field) and synthetic data, respectively. Table 2 compares the statistical properties of the water equivalent of synthetic, natural, and adjusted snow cover. The data show that the adjusted snowfield has the fractal properties of the synthetic snowfield (indexed by the Hurst exponent) and the frequency characteristics of the natural snow cover (indexed by the mean and standard deviation).

Table 1. Coefficients of Variation of Snow Water Equivalent for Describing the Frequency Distribution of Snow Water in Late Winter on Various Landscapes in a Prairie Environment by a Lognormal Distribution

Landform	Sample Size*	CV_{SWE}
Fallow		
Flat plains; slightly to moderately rolling topography with gentle slopes	100	0.47
Bottom (bed) of wide waterways; large sloughs and depressions	3	0.30
Crests of hills, knolls, and ridges	24	0.58
Stubble		
All landforms	126	0.33
Pasture		
Flat plains; bottom (bed) of wide waterways; large sloughs and depressions; slightly to moderately rolling topography with gentle slopes	40	0.41
Crests of hills, knolls, and ridges	14	0.51
Lee of abrupt, sharp slopes	12	0.57
Scattered Brush		
Bottom (bed) of waterways, e.g., gullies; sloughs and depressions	30	0.42
Lee of abrupt sharp, slopes	27	0.52
Yards		
...	3	0.50

*Number of data sets, each containing between 30 and 78 point measurements sampled at a depth:density ratio of 6:1 or less, that were used for the determination of CV.

4. Comparison of Synthetic and Natural Snow Patches

The procedures and findings above were tested by comparing the geometries of soil and snow patches formed by the ablation of synthetic and natural snow covers. The measured data were obtained from image analyses of aerial photographs taken during snowmelt of the depletion in a snow-covered area on a small (1.9 km^2) watershed in the prairie region of west-central Saskatchewan, Canada. The catchment, Smith Tributary, drains an upland area of flat and slightly rolling topography that is under cultivation for the production of cereal grains by dryland farming. Unlike many watersheds in the region, Smith Tributary contains an extensive, well-developed drainage system. Its main drainage ways are deeply incised and act as major areas for the accumulation of wind-transported snow. The primarily vegetation on the channel slopes is native prairie

Table 2. Properties of Synthetic, Natural, and Adjusted Synthetic Snowfields

Statistic	Synthetic (Initial)	Natural (Measured)	Synthetic (Adjusted)
Hurst exponent*	0.90	1.22	0.90
$\overline{SWE_s}$, mm	23.44	8.76	8.71
s, mm	5.03	3.01	2.96

*The Hurst exponent [*Feder*, 1988] is a measure of fractal structure. Values for the exponent near 0.5 indicate random spatial distribution; larger values indicate fractal structure.

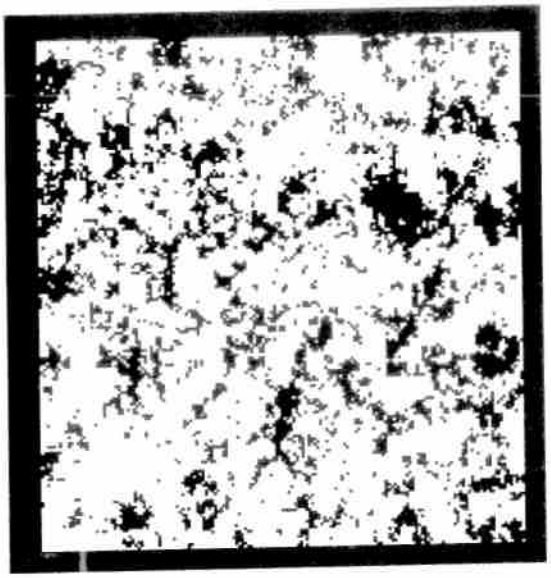

Figure 8. Image of a partially ablated, synthetic snow cover.

grass and shrubs. Through using land use and topographical information, the watershed area was divided into three of the land use–landform classes identified in Table 1: fallow (flat plains, slightly to moderately rolling topography), 20%; stubble (all landforms), 35%; scattered brush and prairie grass (bottom of waterways), 45%, with coefficients of variation of water equivalent of 0.47, 0.33, and 0.42, respectively.

A synthetic snow cover was generated by the FSP process for each land unit in an array containing up to 40,000 elements. The synthetic snowfield was adjusted by (5) for each landscape class using the selected CV_{SWE} and an estimate of the mean snow water equivalent established from point field measurements. Then each array was scaled according to the area of its landscape class. The snow covers on the various arrays were melted by a modified version of energy budget snowmelt model [*Gray and Landine*, 1988; *Granger and Gray*, 1990] in the prairie snow cover ablation simulation (PSAS) [*Shook et al.* 1993b; *Shook*, 1995] using climatological measurements monitored at a station adjacent to the Smith Tributary. At various stages of ablation the perimeters and areas of the soil and snow patches were measured. To determine the snowfield on a given day, the perimeters and sizes of patches on each landscape class were calculated and combined. Figure 8 shows a typical image of a partially ablated, synthetic snow cover.

Since the soil and snow patches of the synthetic and natural snow covers behave as fractal objects, the agreement of their geometries can be tested through comparisons of their fractal dimension(s). The fractal dimension(s) were determined from the perimeter-area and area-frequency characteristics using the power equations given by *Mandelbrot* [1982]:

Perimeter-area:

$$P = kA^{D_p/2}, \tag{6}$$

where

P perimeter;
k constant;
A area;
D_p fractal dimension (values of $D_p > 1.0$).

Korčak's law is a rule of thumb that has been found to apply to many fractal systems. The law states that the areas of natural fractal objects follow a hyperbolic size distribution, that is,

Area-frequency:

$$F(A) = cA^{-D_K/2} \qquad A \geq A_{\min}, \tag{7}$$

where $F(A)$ is fraction of the number of objects with a size equal to or greater than area, A; c is the area of the smallest resolution cell; and D_K is fractal dimension. D_K indexes the degree of concentration of area. A small value indicates that most of the area is concentrated in only a few objects; a large value indicates a uniform distribution of areas.

Figure 9 shows the perimeter-area relationship and Figure 10 shows the area-frequency relationship of ablated snow patches for synthetic and natural snow fields on Smith Tributary when the watershed area is about 62% snow-covered. The data in Figure 9 show close agreement in the perimeter-area relationships of the patches. Conversely, the size-distribution curve for the synthetic snow cover falls above that of natural snow although the slopes of the curves for the patches from the

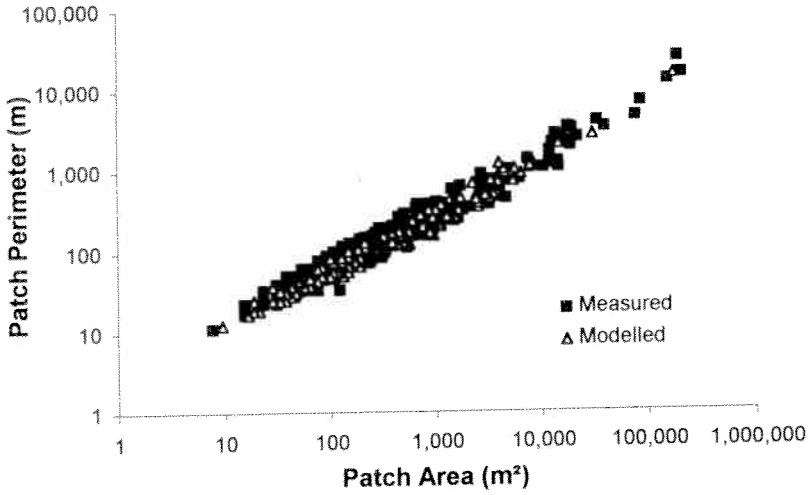

Figure 9. Perimeter-area relationships of snow patches for synthetic and natural snow covers.

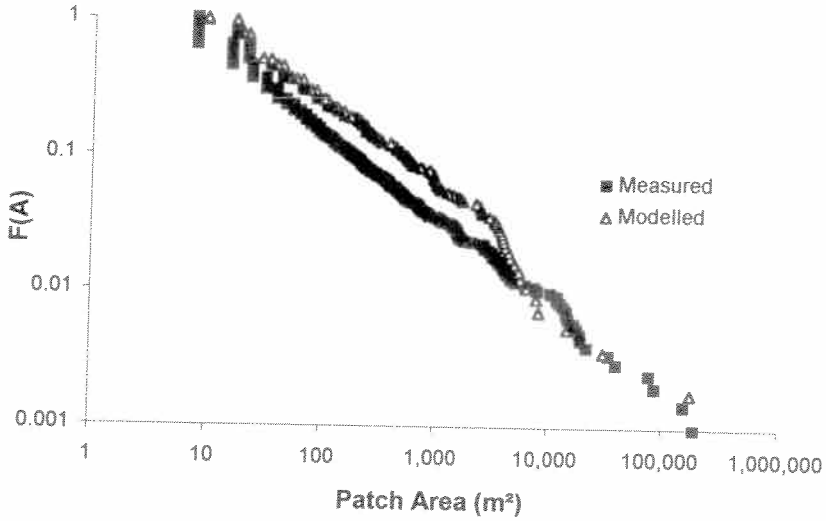

Figure 10. Frequency-area relationships of snow patches for synthetic and natural snow covers.

two snowfields are in reasonable agreement (Figure 10). The higher $F(A)$ by the model is due to the smaller number of grid points used by the model compared to the image analysis system (≈490,000) in deriving the perimeter, area, and number of snow patches. The major effect of higher resolution is to increase the number of small patches that are monitored.

Table 3 lists the fractal dimensions calculated from these data. The data show close agreement of these values for the two snowfields. Therefore it is concluded that synthetic snow covers, which produce ablated snowfields with geometries similar to those of natural snow, can be generated by fractal techniques from information on the water equivalent of a snow cover.

5. Summary

A method of synthesizing the spatial distribution of water for shallow seasonal snow covers of open, exposed environments is developed. The approach is based on the fractal structure of the spatial distribution in the water equivalent, which is due to the autocorrelation of snow depth, the poor association between snow depth and integrated snow density, and the small spatial variations in density compared with depth.

A synthetic snow cover is generated by the method of fractal sum of pulses and placed in an array. The adjustment of the synthetic snow cover to have properties of a natural snow cover is achieved using the two-parameter, lognormal probability density function to describe the frequency distribution of the snow water equivalent. This requires estimates of the mean and the standard deviation or the coefficient of variation of the water equivalent, CV_{SWE}, from field samples. On the prairies, $CV_{SWE} \approx 0.33$ for land with closely spaced, vegetative cover (e.g., wheat stubble), independent of landform; for land in fallow, sparse vegetation, and pasture, CV_{SWE} varies with terrain variables that affect the erosion and deposition of wind-transported snow. For erodible crests of hills, knolls, and ridges, CV_{SWE} typically ranges between 0.50 and 0.60; for low, depressional areas of snow accumulation, CV_{SWE} ranges between 0.30 and 0.45.

Geometrical properties of patches of snow formed by melting a synthetic snow cover are compared to those for a natural snow cover. The fractal dimensions for the synthetic (D_{Ps}, D_{Ks}) and natural (D_{Pn}, D_{Kn}) snow covers, derived from the area-perimeter and size-frequency characteristics of the snow patches with an area about 62% snow-covered were $D_{Ps} = 1.36$, $D_{Pn} = 1.35$ and $D_{Ks} = 1.27$, and $D_{Kn} = 1.31$, respectively.

The procedure enables a hydrologist to synthesize a snowfield from few field data. Melting of the snow cover offers a rational approach for (1) defining source and contributing areas of snowmelt, runoff, and infiltration and (2) accounting for the effects of depletion in snow-covered area on the radiation balance and the effects of local advection of energy on snowmelt and evaporation.

Table 3. Fractal Dimensions, D_P and D_K, of Snow Patches due to Ablation of Synthetic and Natural Snow Covers on Smith Tributary: 62% Snow Cover

	Perimeter-Area		Size-Frequency	
Snow Cover	D_P	r^2	D_K	r^2
Synthetic	1.36	0.99	1.27	0.98
Natural	1.35	0.99	1.31	0.98

Here r^2 is the coefficient of determination.

Acknowledgments. The authors wish to acknowledge the financial support provided the study by the Natural Science and Engineering Research Council of Canada through their Operating and Strategic Grants programs. Special thanks are also directed to Dell Bayne, Research Technician, for his contributions in the collection, tabulation, and processing of snow data. The authors express their appreciation to the reviewers of the manuscript for the constructive comments and suggestions. These recommendations improved significantly the clarity and readability of the paper.

References

Anderson, E. A., National weather service river forecast system–snow accumulation and ablation model, *NOAA Tech. Memo. NWS HYDRO-17*, 1973.

Buttle, J. M., and J. J. McDonnell, Modelling the areal depletion of snowcover in a forested catchment, *J. Hydrol., 90*, 43–60, 1987.

Chow, V. T., The log-probability law and its engineering applications, *Proc. Am. Soc. Civ. Eng., 80*(536), 1–25, 1954.

Dunne, T., and L. B. Leopold, *Water in Environmental Planning*, W. H. Freeman, New York, 1978.
Feder, J., *Fractals*, Plenum, New York, 1988.
Ferguson, R. J., Magnitude and modelling of snowmelt in the Cairngorm mountains, *Hydrol. Sci. J.*, *29*, 49–62, 1984.
Gleick, J., *Chaos: Making a New Science*, Viking, New York, 1987.
Granger, R. J., and D. M. Gray, A net radiation model for calculating daily snowmelt in open environments, *Nord. Hydrol.*, *21*, 217–234, 1990.
Gray, D. M., and P. G. Landine, An energy-budget snowmelt model for the Canadian Prairies, *Can. J. Earth Sci.*, *25*(8), 1292–1303, 1988.
Lovejoy, S., and B. B. Mandelbrot, Fractal properties of rain, and a fractal model, *Tellus Ser. A*, *37*, 209–232, 1985.
Mandelbrot, B. B., *The Fractal Geometry of Nature*, W. H. Freeman, New York, 1982.
Martinec, J., Limitations in hydrological interpretations of the snow coverage, *Nord. Hydrol.*, *11*, 209–220, 1980.
Martinec, J., Snowmelt-runoff models for operational forecasts, *Nord. Hydrol.*, *16*, 129–136, 1985.
McKay, G. A., Precipitation, in *Handbook on the Principles of Hydrology*, edited by D. M. Gray, p. 2.34, Secretariat Can Nat. Comm. Int. Hydrol. Decade, Nat. Resour. Council Can., Ottawa, ON, 1970.
Shook, K., Fractal geometry of snowpacks during ablation, M.Sc. thesis, pp. 1–178, Univ. of Sask, Saskatoon, Canada, 1993.
Shook, K., Simulation of the ablation of prairie snowcovers, Ph.D. thesis, pp. 1–189, Univ. of Sask, Saskatoon, Canada, 1995.
Shook, K., and D. M. Gray, Determining the snow water equivalent of shallow prairie snowcovers, paper presented at 51st Eastern Snow Conference, Dearborn, Mich., June 14–16, 1994.
Shook, K., and D. M. Gray, Small-scale spatial structure of shallow snowcovers, *Hydrol. Processes*, in press, 1997.
Shook, K., D. M. Gray, and J. W. Pomeroy, Temporal variation in snowcover area during melt in Prairie and Alpine environments, *Nord. Hydrol.*, *24*, 183–198, 1993a.
Shook, K., D. M. Gray, and J. W. Pomeroy, Geometry of patchy snowcovers, paper presented at 50th Eastern Snow Conference, Quebec City, Quebec, Canada, June 8–10, 1993b.
Steppuhn, H., and G. E. Dyck, Estimating true basin snowcover, *Advanced Concepts and Technology in the Study of Snow and Ice Resources*, pp. 314–328, Natl. Acad. Sci., Washington, D. C., 1974.
Tabler, R. D., and R. A. Schmidt, Snow erosion, transport and deposition, in *Proceedings of Symposium on Snow Management for Agriculture, Great Plains Agric. Counc. Publ. 120*, edited by H. Steppuhn and W. Nicholaichuk, pp. 12–58, Univ. of Nebr., Lincoln, 1986.
Turcotte, D. L., *Fractals and Chaos in Geology and Geophysics*, Cambridge Univ. Press, New York, 1992.
U.S. Army Corps of Engineers, Snow hydrology: Summary report of the snow investigations, 437 pp., N. Pac. Div., U.S. Army Corps of Eng., Portland, Oreg., 1956.
Woo, M. K., and P. Marsh, Determination of snow storage for small eastern high Arctic basins, paper presented at 34th Eastern Snow Conference, Belleville, Ontario, Canada, Feb. 3–4, 1977.

D. M. Gray and K. Shook, Division of Hydrology, University of Saskatchewan, 57 Campus Drive, Saskatoon, SK S7N 5A9. (e-mail: kshook@duke.usask.ca)

(Received July 15, 1996; revised November 4, 1996; accepted November 13, 1996.)